ELSEVIER

Chemical Engineering Journal 70 (1998) 189–195

Chemical Engineering Journal

Dynamics of pressure build-up accompanying multicomponent gas transport in porous solids: inert gases

Vladimír Hejtmánek *, Pavel Čapek, Olga Šolcová, Petr Schneider

Institute of Chemical Process Fundamentals, Academy of Sciences of the Czech Republic, Rozvojová 135, 165 02 Praha 6-Suchdol, Czech Republic

Received 1 September 1997; received in revised form 30 March 1998; accepted 18 April 1998

Abstract

The dynamics of countercurrent transport of binary and ternary gas mixtures through a porous medium accompanied by a spontaneous temporary build-up of pressure inside the porous medium was experimentally studied. From the measurements, it follows that if a lighter gas replaces a heavier gas the pressure increases and vice versa. The larger the difference between molecular weights of the transported gases the larger the change of the pressure. The spontaneous pressure build-up can be satisfactorily described by the Mean Transport Pore Model (MTPM) or the Dusty Gas Model (DGM). Both models contain three parameters (transport parameters), which represent material constants of the porous medium, i.e., are independent of the kind of transported gases and conditions under which the transport takes place (temperature, pressure). Transport parameters have to be determined experimentally, e.g., by measurements similar to those performed in this study. With the use of obtained transport parameters it is possible to predict the transport under different conditions.

Keywords: Dynamic transport; Multicomponent; Transport parameters; MTPM; DGM

1. Introduction

It is often believed that when a porous solid filled with a gas or a gas mixture is suddenly placed in another gas or gas mixture environment, the gas transport in the pores is purely diffusional, i.e., the situation in pores is isobaric. Similarly, isobaric conditions in pores are assumed during, e.g., a catalytic reaction taking place on pore walls under steady-state conditions. In general this is, however, not true. Isobaric diffusion in pores is possible only when the Graham law is fulfilled. For a n-component gas mixture the generalized Graham law reads

$$\sum_{i=1}^{n} N_i^{\mathrm{d}} \sqrt{M_i} = 0 \qquad (1)$$

(N_i^{d} and M_i are the diffusion molar flux density of gas mixture component i and the molecular weight of this component). This law is violated during the dynamic process of changing the composition of the gas (gas mixture) surrounding the porous solid. During a catalytic reaction the molar flux densities of gas mixture components are, obviously, related by the reaction(s) stoichiometry and not by the Graham law. Only in a hypothetical case when all the mixture components are of equal molecular weights, Eq. (1) could be fulfilled. Violation of the Graham law is reflected by a spontaneous change (increase/decrease) of the total pressure in different places of pores. Under dynamic conditions this pressure change is also time dependent. This was first experimentally verified by Asaeda et al. [1] in their study of inert gas transport ($H_2/N_2/Ar$) in a bed packed with fine glass powder. Recently, the transient pressure and concentration changes in porous samples typical for heterogeneous catalysts were studied by Novák et al. [2] and Arnošt and Schneider [3].

Thus, in addition to the diffusion transport (with mole fraction, i.e., composition, gradient as the driving force, $\mathrm{d}y_i/\mathrm{d}x$) the permeation transport (with total pressure gradient as driving force, $\mathrm{d}p/\mathrm{d}x$) starts to operate and has to be taken into account.

Investigation of the dynamics of gas transport in porous solids has an impact on many chemical engineering situations. Start-up and switching-off catalytic reactors, adsorption processes on porous adsorbents and random steady-state fluctuations in these processes can be named as examples. The knowledge of the qualitative features of the combined transport and the ability to describe its dynamics is of basic importance for the process design and choice of optimum reactor and adsorber regimes.

* Corresponding author. E-mail: schneider@icpf.cas.cz

1385-8947/98/$ - see front matter
PII S1385-8947(98)00095-3

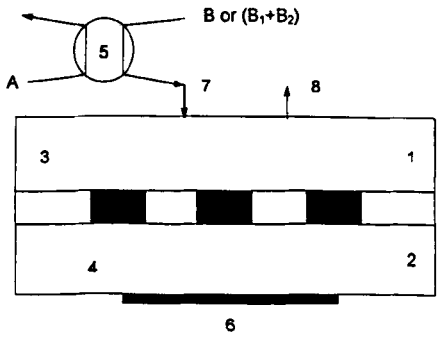

Fig. 1. Scheme of the measuring cell: (1) upper compartment, (2) lower compartment, (3) porous pellets, (4) impermeable disc, (5) four-way valve, (6) pressure transducer, (7) cell inlet, (8) cell outlet.

We have studied the dynamics of combined permeation and diffusion transport in an industrial porous catalyst with binary and ternary mixtures of inert gases:

1. to show qualitatively how the total pressure changes develop and
2. to develop a rational description of dynamics of the combined gas transport in porous catalysts and adsorbents.

The diffusion cell, shown schematically in Fig. 1, was used for the determination of dynamic pressure responses to step changes of gas composition. The studied cylindrical porous pellets were mounted in cylindrical holes of the otherwise impermeable metallic disc, which separated the upper flow-through cell chamber from the closed bottom chamber. The closed cell chamber was equipped with a sensitive pressure transducer. By flowing a gas or gas mixture (A) through the upper compartment, before the start of measurement, *both* cell chambers were filled with A. At the measurement start the gas or gas mixture (A) in-flow into the upper compartment was step-wise replaced by gas or gas mixture B (denoted as $B \rightarrow A$; if both gases were reversed $A \rightarrow B$). Output of the pressure transducer was followed until the pressure before the measurement start was restored. Different pairs $B \rightarrow A$ were selected from the set of four inerts: hydrogen, helium, nitrogen, argon. To study ternary gas transport binary gas mixtures (B_1+B_2 or A_1+A_2) of hydrogen, helium, nitrogen or argon [denoted as $(B_1+B_2) \rightarrow A$ or $(A_1+A_2) \rightarrow B$] containing 25, 50 and 75 vol.% of one component were used.

2. Experimental

2.1. Catalyst

Cylindrical pellets (height/diameter = 3.81/5.50 mm) of a commercial Imperial Chemical Industries catalyst ICI 52/1 was used. Textural properties of the tested catalyst are summarized in Table 1. From the pore-size distributions (Fig. 2) obtained by a combination mercury porosimetry (AutoPore 9200, Micromeritics, USA) and low temperature nitrogen adsorption (DigiSorb 2600, Micromeritics, USA) can be seen that the catalyst is monodisperse.

Table 1
Textural properties of catalyst ICI 52/1

Specific surface	73 m^2/g
Skeletal density	3.833 cm^3/g
Apparent density	1.518 cm^3/g
Pore volume	0.377 cm^3/g
Porosity	0.604
Mean pore diameter	16.4 nm

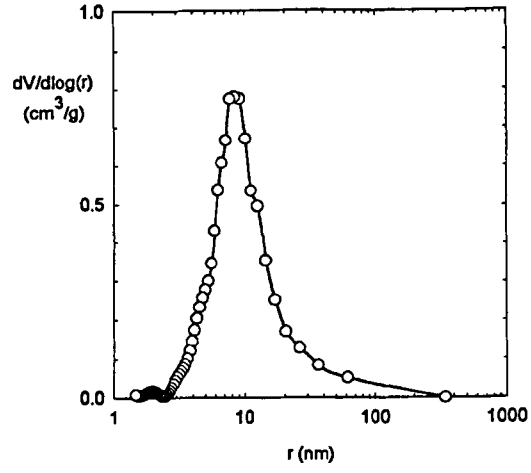

Fig. 2. Pore size distribution of ICI 52/1.

2.2. Gases

Gases (hydrogen, helium, nitrogen and argon; Linde) from pressure cylinders had the 0.9995% purity.

2.3. Diffusion cell (Fig. 1)

The cylindrical pellets of ICI 52/1 (48 pieces) were fastened into the holes of the metallic disc by forcing them first into an undersized silicon rubber tube and then forcing the pellet-rubber tube assembly into the hole.

The pressure transducer (type 4-API-50; Jumo Wien, Austria) responded linearly in the pressure range −100 to +50 kPa. The volume of the lower cell compartment was minimized (10.2 cm^3) to achieve shortening of the responses. The volume of the upper cell compartment was 9.1 cm^3. The flow-rates of gases entering the upper cell compartment were adjusted by mass flow-meter controllers (type 306 KA/RA; Tesla Rožnov, Czech Republic). A four-way valve was used for switching of gases entering the upper compartment. The gas flow rate in the upper cell compartment was maintained approximately at 1.3 cm^3/s.

Readings from the pressure transducer were stored in a computer and transformed into relative pressures $p_{rel} = p/p_b$ (where p_b is the atmospheric pressure).

All the experimental runs were carried out at laboratory pressure and temperature.

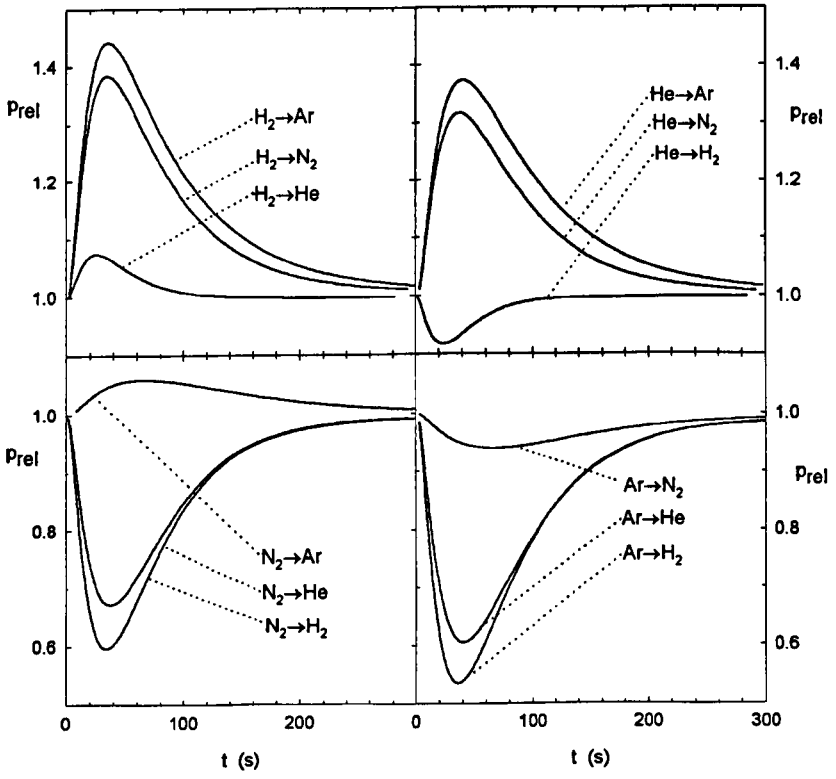

Fig. 3. Response of some binary systems.

3. Pressure dynamics

3.1. Binary systems

Fig. 3 shows the time developments of relative pressure responses for all binary combinations of the four inert gases employed.

As can be seen, the higher the difference between molecular weights of both gases, the more pronounced the extreme of the $p_{rel}(t)$ dependence. Of interest is also the absolute value of the extreme. For the cases where light gas replaces the heavy gas (i.e., hydrogen or helium replacing nitrogen or argon) the maximum on $p_{rel}(t)$ represents 30–50% of the initial pressure. On the other hand, when light gas replaces another light gas (i.e., hydrogen with helium), or, when a heavy gas replaces another heavy gas (i.e., nitrogen with argon) the height of the extreme of $p_{rel}(t)$ amounts to less than 10%. Naturally, the smaller the height of the $p_{rel}(t)$ extreme the shorter the response.

It should be also noticed that the $p_{rel}(t)$ responses for cases $B \rightarrow A$ are not exact mirror images of reversed systems $A \rightarrow B$. This is demonstrated in Fig. 4 for step changes $H_2 \rightarrow N_2$ and $N_2 \rightarrow H_2$. In order to make the comparison more clear ($2\text{-}p_{rel}(t)$) is plotted instead $p_{rel}(t)$ for systems where heavier gas replaces lighter gas ($N_2 \rightarrow H_2$, $Ar \rightarrow He$). Besides the differences between heights of response extremes, there exists also a small difference in response tail parts.

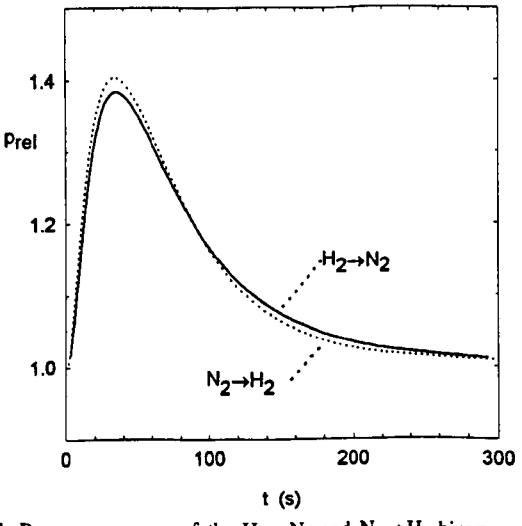

Fig. 4. Pressure response of the $H_2 \rightarrow N_2$ and $N_2 \rightarrow H_2$ binary systems. Response of the $N_2 \rightarrow H_2$ binary is plotted as $2\text{-}p_{rel}$.

3.2. Ternary systems

Thirty responses were obtained for binary mixtures replacing single gases, $(B_1 + B_2) \rightarrow A$, and single gases replacing binary mixtures, $A \rightarrow (B_1 + B_2)$. The binary mixtures contained 25, 50 and 75 vol.% of gas B_1. In the binary mixture combinations light gas B_1 (H_2, He) and heavy gas B_2 (N_2, Ar) were always preferred. The results for systems $(H_2 + N_2) \rightarrow Ar$, $Ar \rightarrow (H_2 + N_2)$, $H_2 \rightarrow (He + Ar)$,

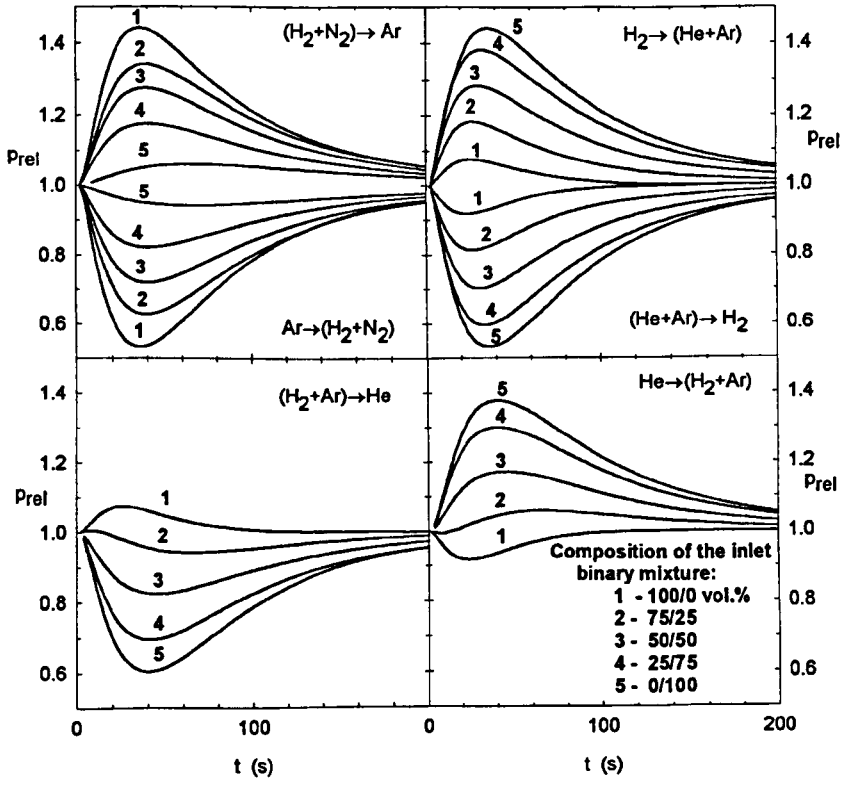

Fig. 5. Pressure responses of ternary systems.

$(He+Ar)\rightarrow H_2$, $(H_2+Ar)\rightarrow He$ and $He\rightarrow(H_2+Ar)$ are depicted in Fig. 5. In all cases the increase in the content of the heavy gas in the inlet binary mixture, B_2, causes an increase of the $p_{rel}(t)$ extreme, i.e., an increase of $(p_{rel})_{max}$ for step changes for which $p_{rel}>1$ and a decrease of $(p_{rel})_{min}$ for which $p_{rel}<1$. The height of the $p_{rel}(t)$ extreme changes nearly linearly with the composition of the inlet binary mixture. This is clearly seen in Fig. 6 for ternary systems $(H_2+Ar)\rightarrow He$ and $He\rightarrow(H_2+Ar)$.

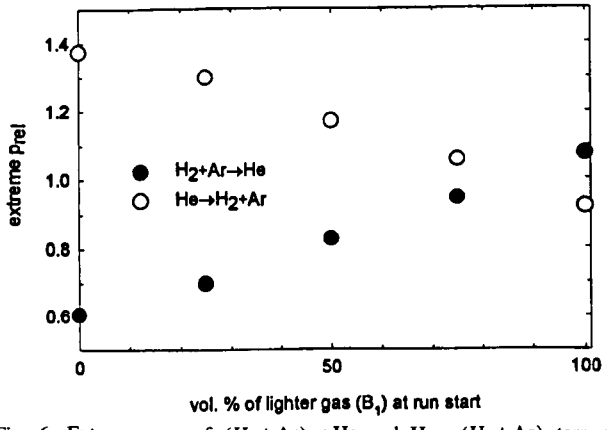

Fig. 6. Extremes p_{rel} of $(H_2+Ar)\rightarrow He$ and $He\rightarrow(H_2+Ar)$ ternary systems.

4. Theoretical

4.1. Models of porous structure

Two models of porous structure are available in the literature for description of the combined transport of multicomponent gas mixtures, viz. the Mean Transport Pore Model (MTPM [4]) and Dusty Gas Model (DGM [5]). Both models are based on the modified Maxwell–Stefan diffusion equation and the Darcy equation describing the permeation flow, i.e., flow under total pressure gradient. The Maxwell–Stefan diffusion equation accounts for diffusive transport in the transition region between the Knudsen region and bulk region. In MTPM the composition gradient (mole fraction gradient) is taken as the diffusion driving force. DGM assumes that diffusion is driven by concentration gradient (gradient of molar concentrations). The permeation equation in the form of Darcy law can take into account either only the Poiseuille viscous flow (DGM), or, combined Knudsen flow, slip at the pore wall and the Poiseuille viscous flow (MTPM: Weber equation [4,6]).

In MTPM, it is assumed that for gas transport the significance of all pore sizes is not the same. The decisive part of the gas transport takes place at the transport-pores (with mean radius $\langle r\rangle$, mean of the squared pore radii $\langle r^2\rangle$, porosity ε_t and tortuosity q_t of the transport pores; ε_t and q_t appear always as ratio which will be denoted as $\psi=\varepsilon_t/q_t$).

DGM is based on the concept of giant 'dust' particles, which form the $(n+1)$-th component of a mixture of n gases.

The kinetic theory of gases is then applied together with the assumption of an external force, which keeps the dust particle immobile.

For both models the relation between the vector of molar flux densities $N=\{N_1, N_2,\ldots, N_n\}^T$ and gradients of molar concentrations has the same form

$$\mathbf{H}\cdot N+\frac{\partial c}{\partial x}=0 \tag{2}$$

where c is the vector of the molar concentrations, $c=\{c_1, c_2,\ldots, c_n\}^T$ and $\mathbf{H}$ is a n^*n square matrix. The concentration dependent elements of this matrix include the transport properties of the pure gases and their binary mixtures and quantities which determine the structure of the porous solid. The elements are defined as

$$h_{ii}=1/D_i^k+(c_i\alpha_i/D_i^k)+\sum_{s=1}^{n}(c_s/c_T D_{is}^m)$$

$$h_{ij}=c_i\alpha_i/D_j^k-c_i/(c_T D_{ij}^m)\quad i\neq j \tag{3}$$

where D_{ij}^m is the effective bulk diffusion coefficient and D_i^k is the effective Knudsen diffusion coefficient, c_T stands for the total molar gas mixture concentration (for perfect gases $p=c_T R_g T$).

MTPM:

$$\alpha_i=\frac{1-\dfrac{B_i}{D_i^k}+\dfrac{1}{c_T}\displaystyle\sum_{s=1,\,s\neq i}^{n}\frac{c_s(B_s-B_i)}{D_{is}^m}}{\displaystyle\sum_{s=1}^{n}\frac{c_s B_s}{D_s^k}}\quad i=1,\ldots,n \tag{4}$$

DGM:

$$\alpha_i=-\frac{B/D_i^k}{c_T+B\displaystyle\sum_{s=1}^{n}c_s/D_s^k}\quad i=1,\ldots,n \tag{5}$$

B_i is the effective permeability coefficient of mixture component i ([4,6])

$$B_i=D_i^k\frac{\omega v_i+\mathrm{Kn}_i}{1+\mathrm{Kn}_i}+\frac{\langle r^2\rangle\psi p}{8\eta}\quad i=1,\ldots,n \tag{6}$$

Kn_i denotes the Knudsen number of component i ($\mathrm{Kn}_i=\lambda_i/(2\langle r\rangle)$ with mean free-path length of molecules i in the gas mixture λ_i (see Arnošt and Schneider [3]), ω is a numeric coefficient which depends on the details of Eq. (6) development; usually $\omega=3\pi/16$, $\pi/4$, 0.8, v_i is the square root of the relative molecular weight of the gas mixture component i:

$$v_i=\sqrt{M_i/\sum_{j=1}^{n}y_j M_j} \tag{7}$$

and η is the gas mixture viscosity.

For DGM the effective permeability coefficient, B, in Eq. (5) is identical for all mixture components and has the form

$$B=(\langle r^2\rangle\psi/8)(p/\eta) \tag{8}$$

The effective diffusion coefficients D_{ij} and D_i^k are defined in MTPM with the use of MTPM transport parameters $\langle r\rangle$ and ψ as

$$D_{ij}^m=\psi D_{ij}^m \tag{9}$$

$$D_i^k=2/3\psi\langle r\rangle\sqrt{8R_g T/(\pi M_i)}$$

where D_{ij}^m is the binary bulk diffusion coefficient of the gas pair i–j.

Two of the three transport parameters in DGM are formally identical with ψ and the product $\langle r\rangle\psi$. Hence, Eq. (9) is valid also for DGM.

4.2. Mass balance of diffusion cell

The constitutive Eq. (2) is associated with mass balances inside the porous pellets

$$\varepsilon\frac{\partial c(t,x)}{\partial t}=-\frac{\partial N(t,x)}{\partial x} \tag{10}$$

i.e.,

$$\varepsilon\frac{\partial c}{\partial t}=\frac{\partial}{\partial x}\left(\mathbf{H}^{-1}\frac{\partial c}{\partial x}\right) \tag{10'}$$

where ε and t denote the pellet porosity and time, respectively. The boundary conditions are derived from mass balance (Eq. (11)) of both diffusion cell compartments, neglecting mass transport resistances between pellets and bulk gas. In addition, ideal mixing in both compartments is assumed

$$V_O\frac{\partial c(t,0)}{\partial t}=-\frac{V_p}{L}N(t,0) \tag{11}$$

$$V_L\frac{\partial c(t,L)}{\partial t}=F^0c^0-Fc^0(t,L)+\frac{V_p}{L}N(t,L)$$

where V_O and V_L are the free volumes of the lower and upper compartment, respectively, V_p is the volume of pellets, F^0 and F are the net volumetric gas flow-rates at the inlet and outlet of the upper compartment. The upper compartment volumetric out-flow rate, F, is unknown and can be expressed from the overall mass balance as

$$F=F^0+\frac{V_p}{Lc_T}\sum_{i=1}^{n}N_i(t,L) \tag{12}$$

Initial conditions for the system, Eqs. (2)–(6) and (10)–(12) are formulated as $c(0,x)=c^*$ with the vector of constant component concentrations, $c^*=\{c_1^*, c_2^*,\ldots, c_n^*\}^T$, after flushing the cell by a single gas or gas mixture.

The set of partial differential equations was integrated by method of lines [7], where the discretization of the integral form of Eq. (10) was achieved by dividing the pellet into small volume elements.

The resulting system of ordinary differential equations was solved using the backward differentiation formulas [8]. For fitting the model transport parameters (ψ, $\langle r\rangle\psi$, $\langle r_2\rangle\psi$) by matching the experimental $p_{rel}(t)$ response to the simulated

Table 2
Transport parameter $\langle r\rangle\square$ for pure Knudsen transport

Fitted	$\langle r\rangle\psi$ (nm)
All responses together	2.372
Individual responses (mean)	2.388
95% confidence interval width	0.048

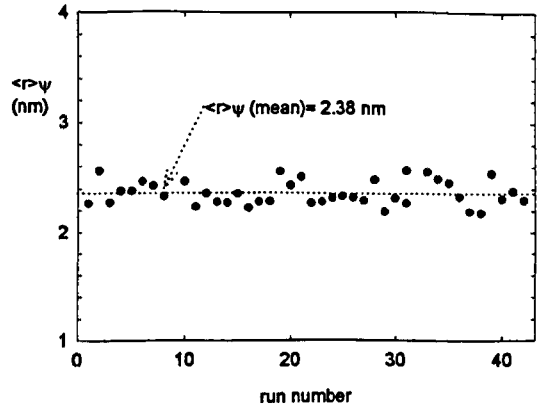

Fig. 7. Optimum $\langle r\rangle\psi$'s for pressure responses of different binary and ternary cases.

response, the sum of squared deviations between experimental and calculated relative pressure was used as the objective function and the simplex algorithm of Nelder and Mead (Himmelblau [9]) as the optimization method. Various combinations of initial parameter guesses and simplex sizes were used to avoid local minima. Parameter fitting was performed both with individual pressure responses as well as with all pressure responses together.

4.3. Transport in the Knudsen region

In the limiting case of very low gas pressure, or very narrow transport pores, i.e., when $\lambda_i \gg \langle r\rangle$, the matrix **H** simplifies to a diagonal form with concentration independent elements

$$h_{ii}=1/D_i^{k} \quad i=1,\ldots,n \tag{13}$$

In this case, only the product of transport parameters $\langle r\rangle\psi$ is needed for pressure response simulation.

5. Simulation and parameter fitting

Both MTPM and DGM were used to determine the set of transport parameters, ψ, $\langle r\rangle\psi$ and $\langle r^2\rangle\psi$. The pair of parameters $\langle r\rangle\psi$ and $\langle r^2\rangle\psi$ reflects the Knudsen and slip contribution to the permeation flow and the pair ψ and $\langle r\rangle\psi$ reflects the role of bulk diffusion and Knudsen diffusion in the net mass transport through the porous medium.

By fitting pressure response for different gas binary and ternary mixtures it was found that the obtained transport parameters were independent of the kind of gases in the mixtures. Also, the differences between the results for MTPM and DGM were negligible. However, the parameter ψ was much higher than unity (ψ= 13.2; mean of ψ for individual pressure responses) inferring transport pore tortuosity $q_t \ll 1$, i.e., a physically meaningless value. At the same time $\langle r^2\rangle\psi$= 0.238 nm^2 pointed out the insignificance of the viscous permeation contribution.

Physically meaningful results were obtained when only the Knudsen transport was considered. In this limiting case, both MTPM and DGM are described by the same set of equations (Eqs. (2) and (10)–(12)) containing only one transport parameter, the product $\langle r\rangle\psi$ (cf. Eq. (9)).

The parameter $\langle r\rangle\psi$ from fitting all pressure responses together and the mean value of this one from fitting individual pressure responses are summarised in Table 2. Fig. 7 shows the random variation of individual optimum $\langle r\rangle\psi$'s which confirms the independence of the transport parameter on the kind of gases used and points to its character of a material constant.

To illustrate the ability of the Knudsen model to predict the pressure responses, the experimental and calculated $p_{rel}(t)$ dependencies for the ternary systems (He + N_2) → Ar and He → (H_2 + Ar) with varying composition of the binary mixtures are shown in Fig. 8. The agreement can be considered as quite satisfactory for both binary and ternary gas mixtures.

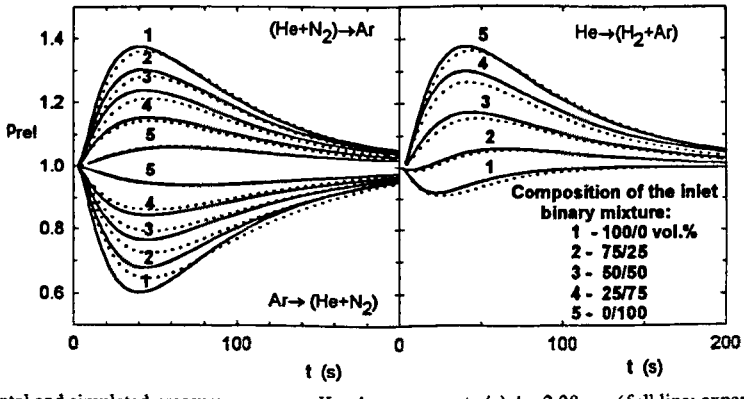

Fig. 8. Comparison of experimental and simulated pressure responses. Knudsen transport: $\langle r\rangle\psi$ = 2.38 nm (full line: experimental; dotted line: calculated).

6. Conclusions

It was experimentally shown that under dynamic conditions the countercurrent transport of binary and multicomponent gas mixtures through a porous medium is accompanied by a spontaneous temporary build-up of pressure inside the porous medium. If a lighter gas replaces a heavier gas the pressure increases and vice versa. The larger the difference between molecular weights of the transported gases the larger the change of the pressure. If one of the gases in the binary case is replaced by a binary mixture (i.e., transport in a ternary gas mixture) the pressure extremes smoothly interpolate between the limiting binary cases.

MTPM or DGM can satisfactorily describe the spontaneous pressure build-up. Both models contain three parameters (transport parameters) which represent material constants of the porous medium, i.e., are independent of the kind of transported gases and conditions under which the transport takes place (temperature, pressure). Transport parameters have to be determined experimentally, e.g., by measurements similar to those performed in this study. With the use of obtained transport parameters it is possible to predict the transport under different conditions.

For the industrial catalyst ICI 52/1, used here, it appeared that the transport pores are very narrow which makes the Knudsen transport dominant. In such a case, only the transport parameters combination $\langle r\rangle\psi$ is of significance. The obtained value $\langle r\rangle\psi=2.38$ nm is very close to $\langle r\rangle\psi=2.55$ nm obtained with the same catalyst under purely diffusion conditions by the chromatographic method [10].

Acknowledgements

The financial support of Grant Agencies of the Czech Republic (# 104/94/1025) and of the Czech Academy of Sciences (# A 472408) is gratefully acknowledged.

Appendix

Nomenclature

B	effective permeability of gas mixture (DGM) (cm^2/s)
B_i	effective permeability of component i (MTPM) (cm^2/s)
$\mathbf{c}$	vector of molar concentrations of mixture components
c_i	molar concentration of component i (mol/cm^3)
c_T	total molar concentration (mol/cm^3)
D_{ij}^m	bulk diffusivity of pair i–j (cm^2/s)
D_{ij}^m	effective bulk diffusivity of pair i–j (cm^2/s)
D_i^k	effective Knudsen diffusivity of component i (cm^2/s)
F^0,F	net inlet and outlet flow-rate of gas mixture (cm^3/s)
$\mathbf{H}$	concentration dependent matrix
h_{ij}	elements of matrix $\mathbf{H}$
Kn_i	Knudsen number of component i (−)
L	pellet length (cm)
M_i	molecular weight of component i (g/mol)
N_i	molar flux density of component i (mol/cm^2 s)
$\mathbf{N}$	molar flux density vector
n	number of gas components
p	pressure (kPa)
q	tortuosity (−)
$\langle r\rangle$	mean transport pore radius (nm)
$\langle r^2\rangle$	mean of squared transport pore radii (nm^2)
R_g	gas constant (J/kmol K)
t	time (s)
V_O, V_L	free volumes of the upper or lower compartment, resp. (cm^3)
V_p	volume of porous pellets (cm^3)
y_i	mole fraction of component
x	length coordinate

Greek symbols

α_i	coefficient
ε	porosity of pellets
ε_t	porosity of transport pores
η	gas mixture viscosity
λ_i	mean free-path length of molecules i
υ_i	square root of the relative molecular weight of component i
Ψ	geometric transport parameter (−)
ω	slip coefficient (−)

References

[1] M. Asaeda, J. Watanabe, M. Kitamoto, J. Chem. Eng. Japan 14 (1981) 129.
[2] M. Novák, K. Erhardt, K. Klusáček, P. Schneider, Chem. Eng. Sci. 43 (1988) 185.
[3] D. Arnošt, P. Schneider, Catalysis Today 20 (1984) 381.
[4] P. Schneider, Chem. Eng. Sci. 33 (1978) 1311.
[5] E.A. Mason, A.P. Malinauskas, Gas Transport in Porous Media: The Dusty-Gas Model, Elsevier, Amsterdam, 1983.
[6] S. Weber, Dan. Mat. Fys. Medd. 28 (1954) 1.
[7] R.F. Sincovec, N.K. Madsen, ACM Trans. Math. Software 1 (1975) 261.
[8] A.C. Hindmarsh, in: R.S. Stapleman et al. (Eds.), ODEPACK, A Systematized Collection of ODE Solvers, in Scientific Computing, North-Holland, Amsterdam, 1983, pp. 55–64.
[9] D.M. Himmelblau, Nonlinear Programming, McGraw-Hill, New York, 1972, p. 148.
[10] O. Šolcová, V. Hejtmánek, P. Schneider, Catalysis Today 38 (1997) 71.